Switching of the core structures of glycosphingolipids from globo- and lacto- to ganglio-series upon human embryonic stem cell differentiation

Yuh-Jin Liang[a], Huan-Hsien Kuo[a,b], Chi-Hung Lin[c], Yen-Ying Chen[c], Bei-Chia Yang[a], Yuan-Yuan Cheng[a], Alice L. Yu[a], Kay-Hooi Khoo[c], and John Yu[a,d,1]

[a]Genomics Research Center, Academia Sinica, Taipei 115, Taiwan; [b]Graduate Institute of Life Sciences, National Defense Medical Center, Taipei 114, Taiwan; and [c]Institute of Biological Chemistry and [d]Institute of Cellular and Organismic Biology, Academia Sinica, Taipei 115, Taiwan

Edited* by Senitiroh Hakomori, Pacific Northwest Research Institute, Seattle, WA, and approved November 23, 2010 (received for review May 26, 2010)

A systematic survey of expression profiles of glycosphingolipids (GSLs) in two hESC lines and their differentiated embryoid body (EB) outgrowth with three germ layers was carried out using immunofluorescence, flow cytometry, and MALDI-MS and MS/MS analyses. In addition to the well-known hESC-specific markers stage-specific embryonic antigen 3 (SSEA-3) and SSEA-4, we identified several globosides and lacto-series GSLs, previously unrevealed in hESCs, including Gb_4Cer, Lc_4Cer, fucosyl Lc_4Cer, Globo H, and disialyl Gb_5Cer. During hESC differentiation into EBs, MS analysis revealed a clear-cut switch in the core structures of GSLs from globo- and lacto- to ganglio-series, which was not as evident by immunostaining with antibodies against SSEA-3 and SSEA-4, owing to their cross-reactivities with various glycosphingolipids. Such a switch was attributable to altered expression of key glycosyltransferases (GTs) in the biosynthetic pathways by the up-regulation of ganglio-series–related GTs with simultaneous down-regulation of globo- and lacto-series–related GTs. Thus, these results provide insights into the unique stage-specific transition and mechanism for alterations of GSL core structures during hESC differentiation. In addition, unique glycan structures uncovered by MS analyses may serve as surface markers for further delineation of hESCs and help identify of their functional roles not only in hESCs but also in cancers.

Glycosphingolipids (GSLs) are lipids containing at least one monosaccharide residue and either a sphingoid or a ceramide (1). They are ubiquitous components of cell membranes and are particularly abundant on surfaces of animal cells. The GSLs in vertebrate animal tissues can be divided generally into three major groups: (*i*) the ganglio- and isoganglio-, (*ii*) the lacto- and neolacto-, and (*iii*) the globo- and isoglobo-series (2, 3). It was suggested that these molecules have important functions as mediators of cell adhesion and signal transduction, and as cell type-specific markers. In vertebrate cells, GSL-enriched surface microdomains organized with various signal transducer molecules seem to be important for modulating cell adhesion and signal transduction (3, 4). In addition, the expressions of GSLs are frequently and drastically changed during development and differentiation; therefore, GSLs are useful as lineage-specific differentiation markers (5–7). Stage-specific embryonic antigen 3 (SSEA-3) and SSEA-4 are considered to be important markers of hESCs, whereas and O4, O1 antigen (8), A2B5 antigens, and GD3 are markers of neural lineage cells (9).

hESCs are pluripotent cells capable of self-renewal and differentiation to form cells of all three germ layers. For years, many studies attempted to unravel the molecular mechanisms that govern hESC pluripotency and differentiation. However, our understanding of the mechanisms regulating the unique capabilities of hESCs is still limited. In particular, the roles of GSLs on the hESC surface are not well elucidated. Although the epitopes defined by the mAbs MC631 (anti-SSEA-3) and MC813-70 (anti-SSEA-4) were delineated (10, 11), the identities and roles of these well-known surface markers for hESCs are mostly not understood. In addition, these antibodies were shown to be cross-reactive to different degrees with various GSLs (10, 11). MC631 recognizes the GalNAcβ1-3Galα1-4Gal epitope, which exists in Gb_5Cer of SSEA-3 and sialyl Gb_5Cer of SSEA-4; it also reacts, to a lesser extent, with Gb_4Cer and the Forssman antigen (GalNAcα1-3Gb_4Cer) and weakly with Globo H (10, 11). On the other hand, the MC813-70 epitope is mostly represented by sialyl Gb_5Cer in SSEA-4. This mAb also cross-reacts to different extents with GM1b and GD1a, and a common structure of the core 1 O-glycan glycoprotein, carrying the NeuAcα2-3Galβ1-3GalNAc epitope (10, 11). Therefore, positive immunostaining with mAbs alone might not necessarily reflect a particular entity of GSLs on hESCs. Instead, a detailed MS analysis coupled with immunostaining is essential to decipher the precise profile of GSLs in hESCs.

Changes in GSLs in mouse ES cells (ESCs) were reported (12–16). However, there are important differences between mouse and human ESCs (17). Whereas most early mouse ESCs are obtained from the inner cell mass before embryo implantation, hESCs are derived from epiblasts of postimplantation embryos (18, 19). In addition, human embryonic carcinoma cell lines that were derived from a teratocarcinoma were also used for similar studies (20, 21). It is well documented that these cells significantly differ from hESCs, not only in the stages of embryonic development but also in the expression of surface markers and growth requirements (22). Furthermore, previous studies often relied on the use of mAbs that recognize glycan epitopes; but these epitopes appear in various glycoconjugates (10).

In this study, we used MALDI-MS and tandem MS (MS/MS) analyses in addition to immunostaining and flow cytometry to systematically delineate changes in expression profiles of GSLs in two undifferentiated hESC lines and 16-d differentiated embryoid body (EB) outgrowth cells. We found that there was a striking switch in the core structures of GSLs from globo- and lacto- to ganglio-series during hESC differentiation. The results not only uncovered several previously unreported glycans in hESCs but also highlighted the value of such combined strategies to overcome the inherent tribulations associated with cross-reactivities of antibodies.

Results

Immunofluorescence and Flow Cytometric Analysis of hESC GSLs. To detect changes in GSLs during hESC differentiation, HES5 cells were induced to differentiate in vitro into EB outgrowth cells for 16 d as described in *Materials and Methods*. Under microscopic observation, human HES5 cells showed high nuclear-cytoplasmic

Author contributions: Y.-J.L., C.-H.L., Y.-Y. Chen, A.L.Y., K.-H.K., and J.Y. designed research; Y.-J.L., H.-H.K., C.-H.L., Y.-Y. Chen, B.-C.Y., and Y.-Y. Cheng performed research; B.-C.Y. and Y.-Y. Cheng contributed new reagents/analytic tools; Y.-J.L., H.-H.K., C.-H.L., Y.-Y. Chen, K.-H.K., and J.Y. analyzed data; and Y.-J.L., C.-H.L., A.L.Y., K.-H.K., and J.Y. wrote the paper.

The authors declare no conflict of interest.

*This Direct Submission article had a prearranged editor.

Freely available online through the PNAS open access option.

[1]To whom correspondence should be addressed. E-mail: johnyu@gate.sinica.edu.tw.

This article contains supporting information online at www.pnas.org/lookup/suppl/doi:10.1073/pnas.1007290108/-/DCSupplemental.

ratios, prominent nucleoli, and compact colony morphology with poorly discernable cell junctions. Once ESCs were induced to differentiate, cells began to organize into 3D aggregates and continued to grow into spherical EB-like structures. After plating onto gelatin-coated culture dishes, human EBs became attached and grew outward to form EB outgrowth cells for a total of 16 d. A typical colony morphology of HES5 cells cultured in the presence of the mouse embryonic fibroblast feeder is shown in Fig. S1*A* (*Left*) In the absence of FGF-2, EB outgrowing cells became attached to the dish surface and migrated radially away from the center of the EB (Fig. S1*A*, *Right*). The morphology of these expanded differentiated cells that grew out of the EBs was highly heterogeneous. Marker analyses with specific antibodies for neurofilaments, nestin (ectoderm), α-smooth muscle actin (mesoderm), and α-fetoprotein (endoderm) showed that differentiated cells from the HES5 cell line expressed markers representative of all three germ layers (Fig. S1*B*). By immunostaining and flow cytometric analysis, populations representing the ectoderm, mesoderm, and endoderm in EB outgrowth cells were estimated to be 68%, 32%, and 4%, respectively (Fig. S1*B*).

To investigate changes in GSLs during hESC differentiation, we initially used mAbs for characterization. GSL-specific antibodies and pluripotency-related Oct3/4 markers were analyzed in undifferentiated hESCs and 16-d differentiated EB outgrowth cells by immunofluorescence microscopy and flow cytometry (Fig. 1). As expected, SSEA-3 was highly expressed in undifferentiated hESCs and down-regulated to ≈3% in differentiated EB outgrowth cells (23). On the other hand, SSEA-4 was also highly expressed in hESCs but decreased to 43% after differentiation to 16-d EB outgrowth cells, as determined by immunostaining (Fig. 1).

Furthermore, Globo H, a hexasaccharide GSL with an α(1,2)-linked fucose that is overexpressed in epithelial cell tumors such as colon, ovarian, gastric, pancreatic, endometrial, lung, prostate, and breast cancers (24, 25), was also detected in undifferentiated hESCs but had almost completely disappeared in differentiated EB outgrowth cells (Fig. 1). To further explore GSL expressions in ESCs and EB outgrowth by flow cytometry, we found that not only globo-series GSLs, such as SSEA-3, SSEA-4, and Globo H, but also a lactose-series GSL, fucosyl Lc_4Cer (H type 1 antigenic determinant), were expressed by hESCs, and these expressions diminished during hESC differentiation (Fig. 1*B*). On the other hand, flow cytometry revealed no substantial difference in the expression of GM1 between ESCs and EB outgrowth cells but significantly higher expressions of GM3 and GD3 in differentiated EB outgrowth cells (Fig. 1*B*).

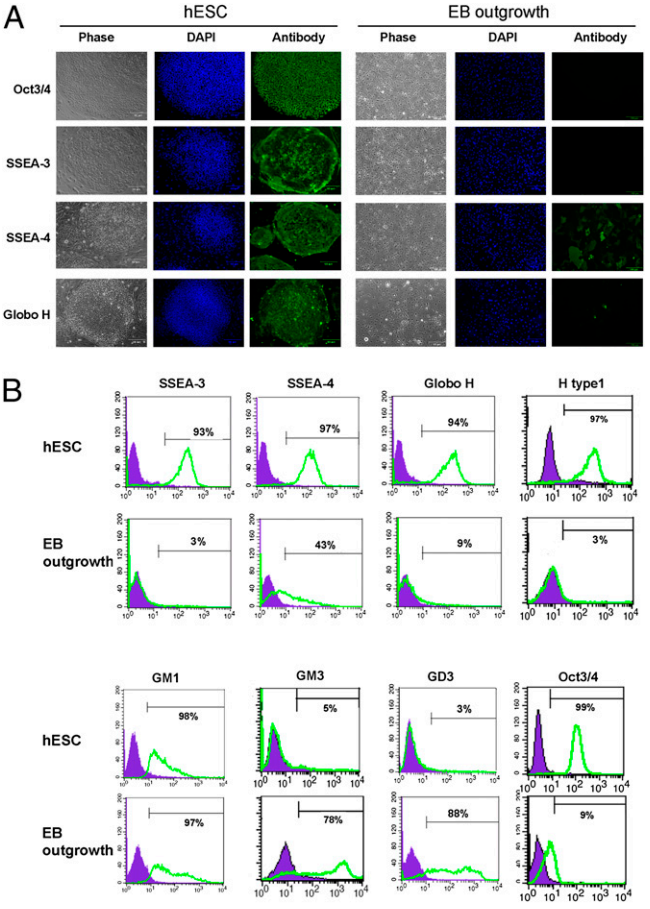

Fig. 1. Analysis of GSL profiles of undifferentiated hESCs and differentiated EB outgrowth by immunofluorescence and flow cytometry. (*A*) Immunofluorescence analysis of GSLs on hESCs and EB outgrowth. (*B*) Flow cytometric analysis of GSLs. SSEA-3, SSEA-4, Globo H, fucosyl Lc_4Cer (using the H type 1 antibody), GM1, GM3, and GD3 were analyzed using GSL-specific antibodies vs. isotype controls. Oct3/4 was analyzed as the control to monitor the undifferentiated status of hESCs. Values represent the mean of three experiments.

MALDI-MS and MS/MS Analysis of hESC GSLs Before and After Differentiation. Previous studies reported various cross-reactivities of mAbs to various GSLs (10, 11), making it difficult to ascertain the presence of particular entities of GSLs on hESCs using mAbs alone. In addition, the cholera toxin B subunit, which we used to detect GM1, was reported to bind GM1 as well as fucosyl GM1, asialo GM1, GD1a, GD1b, GT1b, GM2, and GM3 (26–28). Thus, to decipher a precise profile of GSLs in hESCs, we used MALDI-MS profiling and MS/MS sequencing to systematically analyze GSLs from hESCs and differentiated EB outgrowth cells. The total crude GSL extracts after Folch partitioning were permethylated and subjected to MALDI-MS and MS/MS analyses without further purification. This approach has the advantage of neutralizing all carboxylic groups on sialic acids by methyl esterification, thus allowing simultaneous semiquantitative profiling of both neutral and negatively charged sialylated species. As shown in Fig. 2, the mass spectra obtained for permethylated GSLs from hESCs and EB cells drastically differed, with each being dominated by several major peaks that occurred in signal clusters owing to the expected heterogeneity of the ceramide moieties. On the basis of the *m/z* values for each of the major sodiated molecular ion signals, as fitted to the expected core structures of the three GSL series (globo-, ganglio-, and lacto-) along with the usual range of the most common permutation of sphingosine and fatty acyl chains, the respective GSL profiles were assigned as annotated in Fig. 2, and these assignments were further confirmed by additional MS/MS analyses of each of the major peaks (Fig. 3).

As expected, GSLs from undifferentiated hESCs were found to comprise Gb_5Cer and its sialylated version, respectively corresponding to the overlapping SSEA-3 and SSEA-4 epitopes (Fig. 2*A*). Low-energy collision-induced dissociation (CID) MALDI-MS/MS analyses of these and a series of other GSLs afforded several common ions, indicating similar core structures (Fig. 3). Among these were the ions at *m/z* 548, which revealed the ceramide moiety, and C ions produced through glycosidic cleavages at Glc and Gal of the ubiquitous Gal-Glc disaccharide unit directly extending from the ceramide, which defined the overall glycosyl composition. All globo-series additionally afforded characteristic C/Z double cleavage ions at *m/z* 449 and 653, corresponding to the internal Hex_2 and Hex_3 units derived from the unique globo-backbone of -3Galα1-4Galβ1-4Glc-. The subsequent GalNAcβ1-3 extension from this backbone defines the Gb_4Cer core sequence, which can be identified by the common Y ion at *m/z* 1200, along with B ions that defined R-GalNAc- nonreducing terminal epitopes. Thus, Gb_5Cer, sialyl Gb_5Cer, and fucosyl Gb_5Cer showed B ions at *m/z* 486 (Hex-HexNAc-), 847 (NeuAc-Hex-HexNAc-), and 660 (Fuc-Hex-HexNAc), respectively. The additional C_2 ion at *m/z* 433 (Fuc-Hex-OH) given by the fucosyl Gb_5Cer (Fig. 3*C*) unambiguously located the Fuc substituent in the nonreducing end and therefore was consistent with a Globo H structure. Collectively,

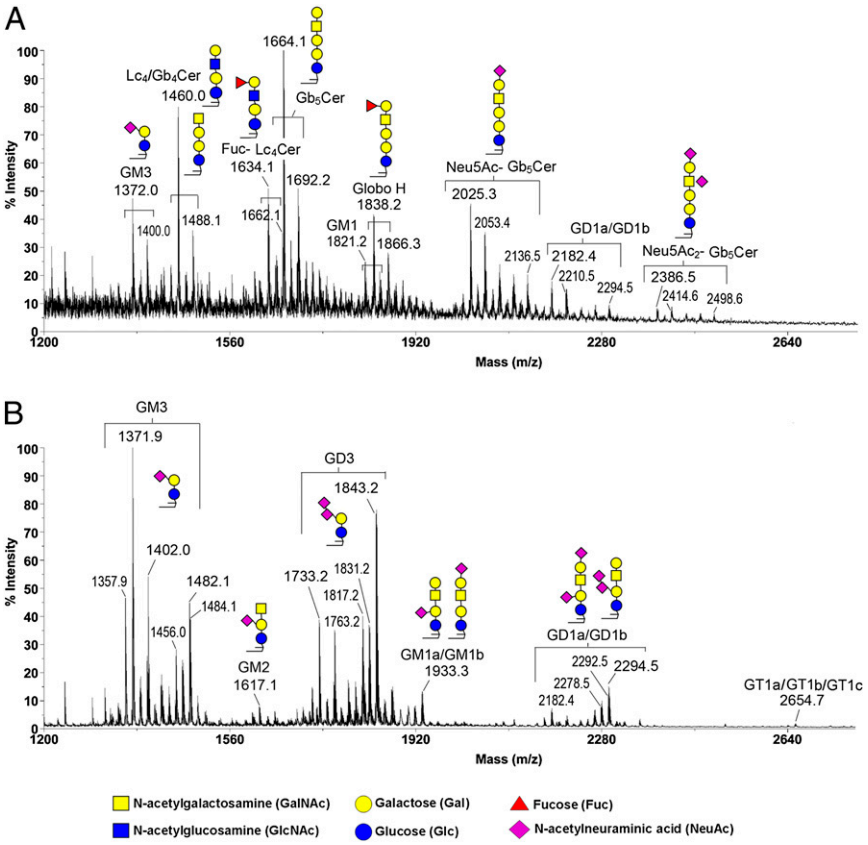

Fig. 2. MALDI-MS profiles of permethylated GSLs from undifferentiated hESCs and differentiated EB outgrowth. (*A*) In addition to Gb_5Cer (SSEA-3) and sialyl Gb_5Cer (SSEA-4), several other globo- and lacto-series GSLs, such as Globo H, disialosyl Gb_5Cer, Gb_4Cer, Lc_4Cer, and fucosyl Lc_4Cer, were present in hESCs. (*B*) In EB outgrowth, the core structures of GSLs had switched to ganglio-series GSLs, giving rise to GM2, GD3, and GD1a/GD1b. Identification of individual GSLs was based on their determined molecular masses and subsequent MS/MS sequencing, facilitated by the knowledge of the core sequences of ganglio-, lacto-, and globo-series and the usual range of fatty acyl heterogeneity associated with the ceramide moiety. Only those GSLs further subjected to MS/MS analyses to confirm their sequence were additionally annotated with illustrations of their major structures. The fatty acyl heterogeneities associated with GSLs from hESCs were primarily C16:0 and C18:0, with a mass difference of 28 u. Only the larger, sialylated GSLs additionally carried longer fatty acyl chains of up to C24:0/C24:1. In contrast, gangliosides from EBs exhibited a more heterogeneous fatty acyl profile, prominently featuring those carrying C24:0/C24:1 (at 112/110 mass units higher than those with C16:0), and those with a hydroxylated C16:0 (at ≥30 u). GSLs with the same glycan moiety but with different fatty acyl contents are bracketed.

these MS/MS data clearly identified the major $[M+Na]^+$ molecular ion signals at *m/z* 1664, 1838, and 2025 as Gb_5Cer (SSEA-3), fucosyl Gb_5Cer (Globo H), and sialyl Gb_5Cer (SSEA-4), respectively, each with the same ceramide moiety corresponding to the most commonly found composition of d18:1 sphingosine and a C16:0 fatty acyl chain. These globo-series can be further extended to include a minor disialylated Gb_5Cer species at *m/z* 2386, which afforded a critical D ion at *m/z* 629 by high-energy CID MS/MS, indicative of an internal NeuAc-HexNAc unit (29) as found in the disialyl terminal motif, NeuAc-Hex-(NeuAc-6)3HexNAc-.

At the lower end, another molecular ion signal at *m/z* 1460 was likewise identified by the Gb-characteristic fragment ions at *m/z* 449, 653, and 1200 as Gb_4Cer; however, additional B and Y ions at *m/z* 486 and 997, respectively, also indicated the presence of a structural isomer corresponding to GSL of the lacto- (or neo-lacto-) series, namely Galßl-3 or Galβ1-4-GlcNAcβ1-3Galβ1-4Glcβ1-1'Cer. Its fucosylated counterpart could be found at *m/z* 1634, with characteristic fragment ions at *m/z* 433 and 660 similar to those afforded by Globo H, indicative of carrying a terminal Fuc-Gal (H antigen) on the Lc_4Cer GSL. The D ion at *m/z* 268 (ΔHexNAc-OH, with the C3-substituent eliminated) afforded by this species under high-energy CID MS/MS further supported the H type 1 epitope, Fuc-Gal-3GlcNAc (Fig. 1*B*), although the data could not rule out the presence of an alternative H type 2 epitope on a neolacto (nLc)-series GSL. More importantly, both the Lc_4Cer and Fuc-Lc_4Cer and all of the identified Gb_4Cer- and Gb_5Cer-related GSLs were clearly down-regulated upon differentiation to the extent that none was detected at any significant level in the permethylated GSL sample from EB cells (Fig. 2*B*). Instead, the latter was dominated by GSLs of the ganglio-series, especially GM3 and GD3.

At first glance, GD3 was only highly expressed in EB cells and not in hESCs, whereas GM3 along with GD1a/GD1b were commonly expressed in both. Other less-abundant ganglio species, including GM2, GM1, and GT1a/GT1b/GT1c, were also more obvious in EB cells, although in general it is not possible to categorically rule out the presence of any of the gangliosides at low amounts in hESCs, which may be suppressed or masked by overlapping, more-abundant signals attributed to the globo-series. Additional MS/MS analyses revealed that isomers of GM1a/GM1b and GD1a/GD1b were present in EB cells.

Interestingly, the most obvious heterogeneity in the ceramide moiety of GM3 and the nonsialylated Gb and Lc in hESCs was represented by molecular ion signals at the 28-u increment, corresponding to a C18 replacing a C16. Only those sialylated Gb_5Cer and GD1a/GD1b/GD1c were additionally accompanied by multiples of 28 u, representing C20, C22, C24, and C24:1 (+110 u from the major species with C16:0), at much lower abundances. In contrast, the ceramide moieties of gangliosides in EB cells were clearly much more heterogeneous. Typically for each of the assigned ganglioside signal clusters, its fatty acyl content was composed of C16 and C16 with an extra OH, C22, C24:1, and C24, among the most abundant components, assuming that each carried the same d18:1 sphingosine base. Thus, even for GD1a/GD1b, which was found in both hESCs and EBs, the relative amounts of species with different fatty acyl contents distinctly differed.

In addition, the results of MALDI-MS indicated that both hESC lines, HES5 and H9, exhibited similar expression patterns of GSLs; moreover, similar patterns of GSL expressions of these hESC lines were determined after their differentiation (Fig. S2).

Alterations in the Expressions of GSL-Related Glycosyltransferases During Differentiation. To elucidate the mechanism underlying alterations in GSLs during hESC differentiation, we analyzed the expressions of glycosyltransferases (GTs) involved in the GSL biosynthetic pathways. The GSL biosynthetic pathways and multiples of changes in expressions of key GTs genes during hESC differentiation are shown in Figs. 4 and 5. First, the Gb_3Cer synthase (*A4GALT*) and Lc_3Cer synthase (*B3GNT5*), which convert the common precursor lactosylceramide to Gb_3Cer and Lc_3Cer, were respectively down-regulated to 30% and 50% of levels in undifferentiated hESCs in differentiated EB outgrowth. In addition, *B3GALT5*, which cat-

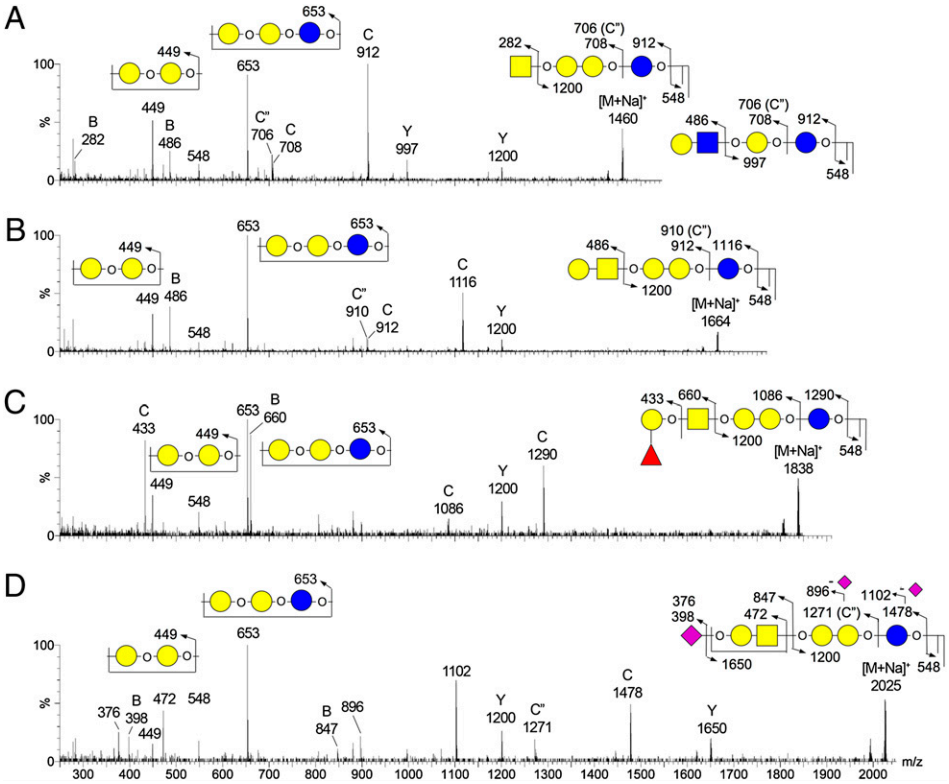

Fig. 3. MALDI CID MS/MS sequencing of permethylated GSLs from undifferentiated hESCs. All detected major peaks were subjected to an MS/MS analysis using both low- and high-energy CID, but for simplicity only four representative low-energy CID MS/MS spectra for globo-series GSLs are shown. (*A*) MALDI CID MS/MS spectrum of m/z 1460 (Gb_4Cer or (n)Lc_4Cer); (*B*) MALDI CID MS/MS spectrum of m/z 1664 (Gb_5Cer); (*C*) MALDI CID MS/MS spectrum of m/z 1838 (Globo H); (*D*) MALDI CID MS/MS spectrum of m/z 2025 (sialyl-Gb_5Cer). A majority of the afforded fragment ions correspond to Y, B, and C ions derived from single or double glycosidic cleavages. C″ ions, as annotated, were commonly observed along with or in place of C ions and occurred at 2 mass units lower than C ions. Assignments of all major fragment ions are illustrated by the embedded illustrations. Only the O atoms at preferred cleavage sites were drawn out to distinguish between B and C or C″ ions.

alyzes SSEA-3 (Gb_5Cer) and Lc_4Cer synthesis, also decreased to 30%, which was attributed to decreases in SSEA-3 and Lc_4Cer expressions in differentiated EB outgrowth. Furthermore, two fucosyltransferases, *FUT1* and *FUT2*, which catalyze the synthesis of Globo H and Fuc-Lc_4Cer, diminished during differentiation (both to 20%). These changes may have led to the inefficient conversion of lactosylceramide to globo- and lacto-series GSLs during hESC differentiation. On the other hand, the conversion of SSEA-3 to SSEA-4 was catalyzed by *ST3GAL1* and *ST3GAL2*, the expressions of which increased by 18.3- and 2.8-fold, respectively. These findings may account for the presence of a residual amount of SSEA-4 in differentiated EB outgrowth cells.

Fig. 5*B* illustrates key GTs involved in the conversion of lactosylceramide toward globo-, lacto-, and ganglio-series GSLs. In contrast to the aforementioned decreases in GTs that are involved in the biosynthesis of globo- and lacto-series GSLs, the GTs involved in the biosynthesis of ganglio-series GSLs, such as GM2 and GM3 synthases (*B4GALNT1* and *ST3GAL5*), respectively increased by 8.4- and 14.2-fold during hESC differentiation. These changes are in line with the increased expressions of gangliosides and reduced expressions of globo- and lacto-series GSLs in differentiated EB outgrowth cells. In addition, expressions of other GTs involved in ganglioside biosynthesis, such as GD3 and GT3 synthases (*ST8SIA1*) and sialyltransferase 4 (*ST3GAL1*), also respectively increased by 8.9-, 8.9-, and 18.3-fold, (Figs. 4*C* and 5*C*). Taken together, alterations of these key GTs may account for the switch in the core structures of GSLs in favor of ganglio-series biosynthesis upon hESC differentiation.

The kinetics of the rise and fall of mRNA levels of GTs was examined during the 16-d course of differentiation of hESCs (Fig. S3). There were initial rapid declines in *B3GALT5*, *FUT1*, and *FUT2* expressions in the first 3 d, followed by subsequent gradual decreases. On the other hand, expressions of *ST3GAL1*, *ST3GAL5*, and *ST8SIA1* showed gradual and steady rises during differentiation. Expressions of *Oct3/4* and *Sox2* genes, which were expected to be down-regulated during hESC differentiation, were used as a control. The results indicated progressive changes in the GT network, which provide a molecular mechanism for modulating the GSL profile on the cell surface during hESC differentiation.

Discussion

GSLs on the surface of mammalian cells have important biological functions in cell adhesion, signal transduction, and differentiation. Yamashita et al. (13) reported that knockdown of the *Ugcg* gene, a key GT for converting ceramide to glucosylceramide in the initial step of the GSL biosynthesis pathway, led to defects in embryonic differentiation after gastrulation, suggesting a vital role of GSL synthesis in development. In addition, using known antibodies, the expressions of several GSLs from mouse ESCs were reported (12–16). However, antibodies that recognize specific glycan epitopes conceivably cross-reacted with various glycoconjugates containing similar defined epitopes (10). Therefore, in this study, profiles of GSLs in two hESC lines and their 16-d differentiated derivatives were examined using MALDI-MS and MS/MS analyses in addition to immunostaining and flow cytometry. Furthermore, Draper et al. (21) reported decreases in SSEA-3 and SSEA-4 and an increase in GD3 during retinoic acid-induced differentiation of hESCs. In this study, in addition to SSEA-3 and SSEA-4, we demonstrated the presence of other globosides and lacto-series GSLs, including Gb_4Cer, Lc_4Cer, fucosyl (n)Lc_4Cer, Globo H, and disialyl Gb_5Cer in hESCs, that were not previously known to be expressed by hESCs. These GSLs expressed by hESCs rapidly diminished upon differentiation to EB outgrowth cells and thus might be useful stage-specific transition markers of hESCs and be valuable for monitoring the properties and behavior of hESCs in culture.

These observations are also consistent with the observed changes in GSL expression patterns during embryonic development of mice (3, 30). On the basis of TLC, the GM1 ganglioside was shown to be present in mouse ESCs (14); furthermore, GM3, GM2, and GD3 were demonstrated using a similar approach (15, 16). In contrast, our studies using hESCs showed that GM3, GM1, and GD1a/GD1b were detected in undifferentiated cells; after differentiation, GM3 and GD1a/GD1b and other gangliosides, such as GM2, GD3, and GT1a/GT1b/GT1c, all increased. In addition,

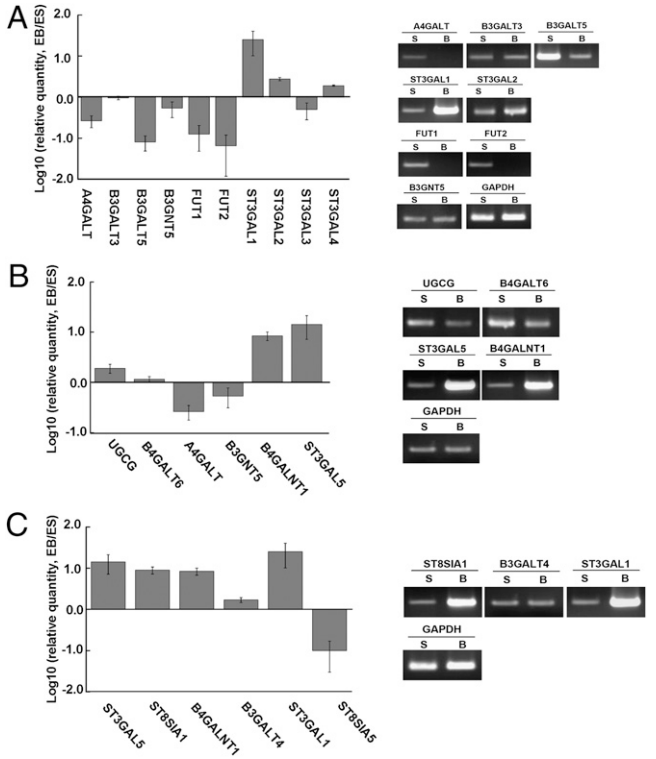

Fig. 4. Expression of GTs involved in the biosynthetic pathway of GSLs. Expression levels of GT genes were analyzed by quantitative RT-PCR. The ratios of EB/ESCs were plotted on a log-scale bar graph. Error bars represent 1 SD from the mean. The RT-PCR products of GT genes were analyzed by agarose gel electrophoresis to confirm the results. (*A*) GTs involved in the synthesis of globo- and lacto-series GSLs. (*B*) GTs involved in the conversion of lactosylceramide, in the initial steps toward the synthesis of all three GSL series. (*C*) GTs involved in the biosynthesis of ganglio-GSLs.

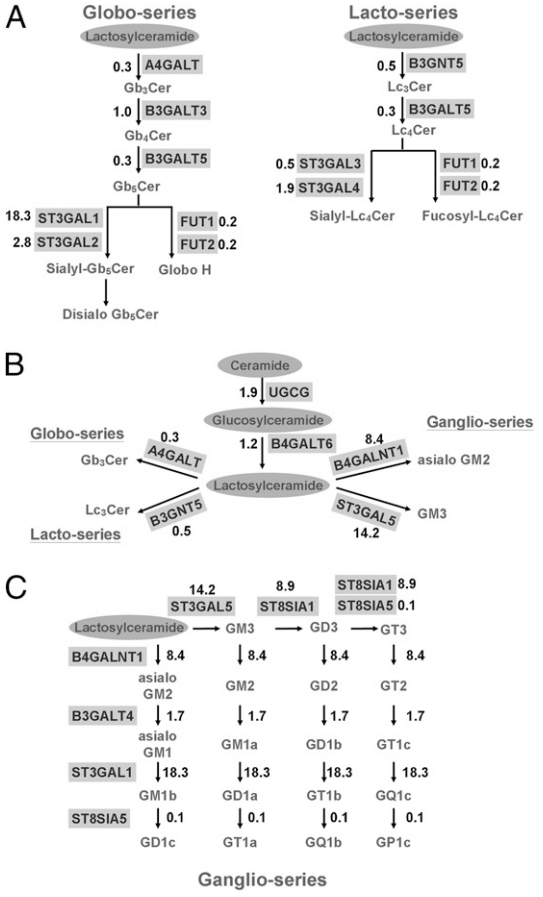

Fig. 5. Alterations of the GTs in various biosynthetic pathways. Various biosynthetic pathways for *A*, *B*, and *C* in Fig. 4 are shown as corresponding diagrams. Numbers in these diagrams represent ratios of expression in EB vs. ESC.

we showed that enzymes responsible for the synthesis of GM2, GD3, and GT1b (i.e., B4GALNT1, ST8SIA1, and ST3GAL1) were up-regulated. Moreover, previous studies using human embryonic carcinoma cells reported that globo-series GSLs prominently expressed by undifferentiated cells shifted to both lacto- and ganglio-series GSLs after retinoic acid-induced differentiation (20). In contrast, we found that in addition to globo-series GSLs, undifferentiated hESCs also expressed lacto-series GSLs including Lc_4Cer and Fuc-(n)Lc_4Cer. Additionally, associated with such expression, Lc3 synthase (B3GNT5) and Lc4 synthase (B3GALT5) were expressed by undifferentiated hESCs but were down-regulated after differentiation. Moreover, it is noted that mAbs against H type 1 antigen, Fucα1-2Galβ1-3GlcNAc, clearly stained the undifferentiated hESCs but not the differentiated EB, confirming the abundance of lacto-series GSLs in hESCs. Recently, Jung et al. (16) reported that in *Ugcg*-suppressed mouse ESCs, there were significant defects in neural differentiation, especially neural maturation related to GFAP and MAP-2 expressions.

It was suggested that cancer cells often possess traits reminiscent of those ascribed to normal early embryonic cells, and on the other hand, cancer cells also express many onco-fetoproteins that are found in hESCs. Thus, these newly found stage-specific glycan entities in hESCs may serve as markers for cancer detection or as targets of cancer therapy. Previously, we reported that SSEA-3, a marker for hESCs, is highly expressed in breast cancer and breast cancer stem cells (31). Another well-known marker of hESCs, SSEA-4, the sialylated derivative of SSEA-3, is also expressed in cancers and breast cancer stem cells (Yu et al., unpublished work). On the other hand, we demonstrated that Globo H, a fucosyl Gb_5Cer overexpressed in many epithelial cell cancers, was highly expressed by undifferentiated hESCs. Recently we reported that the level of epithelial cell adhesion molecule expression that was correlated with dedifferentiation and malignant proliferation of epithelial cells and cancer stem cells was expressed in undifferentiated rather than differentiated hESCs and was associated with maintenance of the undifferentiated phenotype of hESCs (32). Furthermore, microarray studies of gene expressions suggested that histologically poorly differentiated tumors show preferential overexpression of genes normally expressed by ESCs (33).

Our finding of a switch in the core structures of GSLs from globo- and lacto- or neolacto- to ganglio-series during hESC differentiation is consistent with the observed changes in expression patterns of GSLs during mouse embryonic development (3). It was reported that globo-series SSEA-3, SSEA-4, and Globo H are expressed at high levels in four cell stages and then later decline during mouse embryogenesis (3). SSEA-1 is not expressed until the morula stage of mouse embryos (3). In addition, ganglio-series GM3, GD3, GT3, GM2, and GD2 are expressed in later stages upon neural crest formation in mice (6, 34), and GD3, GD1a, and GT1b were also expressed after somite formation (6, 35). Moreover, we demonstrated that GSL alterations could be accounted for by changes in the expressions of key GTs in biosynthetic pathways of GSLs. For example, Gb5 synthase (*B3GALT5*)- and Globo H-related FUT1/FUT2 were significantly suppressed when hESCs differentiated into EB outgrowth cells, accounting for the disappearance of SSEA-3 and Globo H from differentiated cells. Similarly, reductions in FUT1/FUT2 also contributed to decreases in fucosyl Lc_4Cer lacto-series. Substantial declines in the expressions of Gb3 synthase (*A4GALT*) and Lc3/Lc4 synthases (*B3GNT5* and *B3GALT5*) coupled with the striking rises in GM3, GD3, and GM2 synthases in EB outgrowth cells may be responsible for the reduced conversion of

lactosylceramide to globo- and lacto-series GSLs and increased ganglio-series.

We herein propose that the modified expression profile of GSLs from globo- and lacto- to ganglio-series during hESC differentiation is primarily directed by the up-regulation of ganglio-series–dependent GTs with simultaneous down-regulation of globo- and lacto-series–dependent GTs. Whether overexpression or knockdown of a few key GTs may lead to any modulation of hESC behavior remains to be explored. In addition, we envision that some of the unique glycan structures uncovered may serve as markers for hESCs and for cancers.

Materials and Methods

Flow Cytometric Analysis. ES and EB outgrowth cells were subjected to trypsin digestion and resuspended in PBS containing 2% FBS. For cell-surface GSL staining, resuspended cells were incubated with optimal concentrations of the primary antibodies and fluorescent-labeled secondary antibodies and analyzed by FACSCalibur (BD Biosciences). Isotype control antibodies were used as a negative control. Viable cells were gated, and hESC-specific GSL expressions were further analyzed in the gated region. For intracellular antigen staining, cells were fixed with 4% paraformaldehyde and permeabilized with ice-cold methanol before staining. Antibodies used are described in *SI Materials and Methods*.

Immunofluorescence Analysis. For GSL staining, ES and EB outgrowth cells grown on coverslips were fixed in 4% formaldehyde for 30 min and washed with PBS. For cell-surface GSL staining, cells were blocked in 5% goat serum in PBS and incubated with appropriate concentrations of the primary antibody and fluorescent-labeled secondary antibody in PBS containing 1% FBS. Subsequently, DAPI was used for staining for 1 min in PBS with 0.1% Triton X-100. A coverslip was mounted with a drop of mounting medium and sealed with clear nail polish to prevent drying and movement under the microscope. For intracellular antigen staining, cells were permeabilized by adding 0.1% TritonX-100 in blocking buffer before staining with the primary antibody. Antibodies used are described in *SI Materials and Methods*.

MALDI-MS Profiling and MALDI CID MS/MS Analysis. MALDI-MS profiling of permethylated GSLs were performed on an ABI 4700 Proteomics Analyzer (Applied Biosystems) using the 2,5-dihydroxybenzoic acid (DHB) matrix (10 mg/mL in water). Low- and high-energy CID MALDI-MS/MS sequencing was performed on a Q/TOF Ultima MALDI (Waters Micromass) with α-cyano-4-hydrocinnamic acid and a 4700 Proteomics Analyzer using the DHB matrix, respectively, as previously described in detail (29).

ACKNOWLEDGMENTS. This study was supported by grants from the Genomics Research Center and Academia Sinica and by Grant NSC98-3111-B-001-003 from the National Science Council, Taiwan. The Resource Core Facilities was also supported by the same National Science Council grant. MALDI-MS and MS/MS data were acquired at the National Research Program for Genomic Medicine Core Facilities for Proteomics and Glycomics, supported by National Science Council Grants NSC97-3112-B-001-018 and NSC98-3112-B-001-023.

1. Chester MA (1998) IUPAC-IUB Joint Commission on Biochemical Nomenclature (JCBN). Nomenclature of glycolipids—recommendations 1997. *Eur J Biochem* 257:293–298.
2. Hakomori S, Ishizuka I (2006) Glycolipids: Animal. *Encyclopedia of Life Sciences* (John Wiley & Sons Ltd, Chichester, UK).
3. Hakomori S (2008) Structure and function of glycosphingolipids and sphingolipids: Recollections and future trends. *Biochim Biophys Acta* 1780:325–346.
4. Hakomori S (2010) Glycosynaptic microdomains controlling tumor cell phenotype through alteration of cell growth, adhesion, and motility. *FEBS Lett* 584:1901–1906.
5. Yu RK (1994) Development regulation of ganglioside metabolism. *Prog Brain Res* 101: 31–44.
6. Yu RK, Macala LJ, Taki T, Weinfield HM, Yu FS (1988) Developmental changes in ganglioside composition and synthesis in embryonic rat brain. *J Neurochem* 50:1825–1829.
7. Bouvier JD, Seyfried TN (1989) Ganglioside composition of normal and mutant mouse embryos. *J Neurochem* 52:460–466.
8. Sommer I, Schachner M (1981) Monoclonal antibodies (O1 to O4) to oligodendrocyte cell surfaces: An immunocytological study in the central nervous system. *Dev Biol* 83: 311–327.
9. Yanagisawa M, Yu RK (2007) The expression and functions of glycoconjugates in neural stem cells. *Glycobiology* 17:57R–74R.
10. Kannagi R, et al. (1983) Stage-specific embryonic antigens (SSEA-3 and -4) are epitopes of a unique globo-series ganglioside isolated from human teratocarcinoma cells. *EMBO J* 2:2355–2361.
11. Kannagi R, et al. (1983) New globoseries glycosphingolipids in human teratocarcinoma reactive with the monoclonal antibody directed to a developmentally regulated antigen, stage-specific embryonic antigen 3. *J Biol Chem* 258:8934–8942.
12. Kimber SJ, Brown DG, Påhlsson P, Nilsson B (1993) Carbohydrate antigen expression in murine embryonic stem cells and embryos. II. Sialylated antigens and glycolipid analysis. *Histochem J* 25:628–641.
13. Yamashita T, et al. (1999) A vital role for glycosphingolipid synthesis during development and differentiation. *Proc Natl Acad Sci USA* 96:9142–9147.
14. Kwak DH, et al. (2006) Dynamic changes of gangliosides expression during the differentiation of embryonic and mesenchymal stem cells into neural cells. *Exp Mol Med* 38:668–676.
15. Lee DH, et al. (2007) Effects of daunorubicin on ganglioside expression and neuronal differentiation of mouse embryonic stem cells. *Biochem Biophys Res Commun* 362: 313–318.
16. Jung JU, et al. (2009) The roles of glycosphingolipids in the proliferation and neural differentiation of mouse embryonic stem cells. *Exp Mol Med* 41:935–945.
17. Pera MF, Reubinoff B, Trounson A (2000) Human embryonic stem cells. *J Cell Sci* 113: 5–10.
18. Hanna J, et al. (2010) Human embryonic stem cells with biological and epigenetic characteristics similar to those of mouse ESCs. *Proc Natl Acad Sci USA* 107:9222–9227.
19. Tesar PJ, et al. (2007) New cell lines from mouse epiblast share defining features with human embryonic stem cells. *Nature* 448:196–199.
20. Fenderson BA, Andrews PW, Nudelman E, Clausen H, Hakomori S (1987) Glycolipid core structure switching from globo- to lacto- and ganglio-series during retinoic acid-induced differentiation of TERA-2-derived human embryonal carcinoma cells. *Dev Biol* 122:21–34.
21. Draper JS, Pigott C, Thomson JA, Andrews PW (2002) Surface antigens of human embryonic stem cells: Changes upon differentiation in culture. *J Anat* 200:249–258.
22. Yu J, Thomson JA (2008) Pluripotent stem cell lines. *Genes Dev* 22:1987–1997.
23. Lanctot PM, Gage FH, Varki AP (2007) The glycans of stem cells. *Curr Opin Chem Biol* 11:373–380.
24. Bremer EG, et al. (1984) Characterization of a glycosphingolipid antigen defined by the monoclonal antibody MBr1 expressed in normal and neoplastic epithelial cells of human mammary gland. *J Biol Chem* 259:14773–14777.
25. Canevari S, Fossati G, Balsari A, Sonnino S, Colnaghi MI (1983) Immunochemical analysis of the determinant recognized by a monoclonal antibody (MBr1) which specifically binds to human mammary epithelial cells. *Cancer Res* 43:1301–1305.
26. Angström J, Teneberg S, Karlsson KA (1994) Delineation and comparison of ganglioside-binding epitopes for the toxins of *Vibrio cholerae*, *Escherichia coli*, and *Clostridium tetani*: Evidence for overlapping epitopes. *Proc Natl Acad Sci USA* 91:11859–11863.
27. Lauer S, Goldstein B, Nolan RL, Nolan JP (2002) Analysis of cholera toxin-ganglioside interactions by flow cytometry. *Biochemistry* 41:1742–1751.
28. Yanagisawa M, Ariga T, Yu RK (2006) Cholera toxin B subunit binding does not correlate with GM1 expression: A study using mouse embryonic neural precursor cells. *Glycobiology* 16:19G–22G.
29. Yu SY, Wu SW, Khoo KH (2006) Distinctive characteristics of MALDI-Q/TOF and TOF/TOF tandem mass spectrometry for sequencing of permethylated complex type N-glycans. *Glycoconj J* 23:355–369.
30. Hakomori S (2000) Traveling for the glycosphingolipid path. *Glycoconj J* 17:627–647.
31. Chang WW, et al. (2008) Expression of Globo H and SSEA3 in breast cancer stem cells and the involvement of fucosyl transferases 1 and 2 in Globo H synthesis. *Proc Natl Acad Sci USA* 105:11667–11672.
32. Lu TY, et al. (2010) Epithelial cell adhesion molecule regulation is associated with the maintenance of the undifferentiated phenotype of human embryonic stem cells. *J Biol Chem* 285:8719–8732.
33. Ben-Porath I, et al. (2008) An embryonic stem cell-like gene expression signature in poorly differentiated aggressive human tumors. *Nat Genet* 40:499–507.
34. Hakomori S (2000) Cell adhesion/recognition and signal transduction through glycosphingolipid microdomain. *Glycoconj J* 17:143–151.
35. Ngamukote S, Yanagisawa M, Ariga T, Ando S, Yu RK (2007) Developmental changes of glycosphingolipids and expression of glycogenes in mouse brains. *J Neurochem* 103:2327–2341.